Weight and power optimization of steam bottoming cycle for offshore oil and gas installations

Lars O. Nord[a,*], Emanuele Martelli[b], Olav Bolland[a]

[a] *Department of Energy and Process Engineering, Norwegian University of Science and Technology, Trondheim, Norway*
[b] *Department of Energy, Politecnico di Milano, Italy*

Abstract

Offshore oil and gas installations are mostly powered by simple cycle gas turbines. To increase the efficiency, a steam bottoming cycle could be added to the gas turbine. One of the keys to the implementation of combined cycles on offshore oil and gas installations is for the steam cycle to have a low weight-to-power ratio. In this work, a detailed combined cycle model and numerical optimization tools were used to develop designs with minimum weight-to-power ratio. Within the work, single-objective optimization was first used to determine the solution with minimum weight-to-power ratio, then multi-objective optimization was applied to identify the Pareto frontier of solutions with maximum power and minimum weight. The optimized solution had process variables leading to a lower weight of the heat recovery steam generator while allowing for a larger steam turbine and condenser to achieve a higher steam cycle power output than the reference cycle. For the multi-objective optimization, the designs on the Pareto front with a weight-to-power ratio lower than in the reference cycle showed a high heat recovery steam generator gas-side pressure drop and a low condenser pressure.

Keywords: black-box optimization, multi-objective optimization, genetic algorithm, combined cycle, process simulation, heat recovery

Nomenclature

child	child solution vector
f	objective function
LHV	lower heating value (kJ/kg)
m	mass (kg)

*Corresponding author
Email address: lars.nord@ntnu.no (Lars O. Nord)

$\dot{m}$	mass flow rate (kg/s)
N_f	number of objective functions
N_p	population size
N_t	number of solutions used by the binary tournament selection operator
parent	parent solution vector
p	population vector
p_{cond}	condensing pressure (bar)
p_{steam}	live steam pressure (bar)
Q	child population
q	vector in the solution space
$rand$	random number uniformly distributed between 0 and 1
$ratio$	tuning parameter of the crossover operator
RL_{gt}	relative gas turbine load (-)
T	temperature (°C)
T_{steam}	live steam temperature (°C)
W/P	weight-to-power ratio (kg/kW)
x	solution vector
$\dot{W}_{aux}$	auxiliary power (W)
$\dot{W}_{gt}$	gas turbine gross power (W)
$\dot{W}_{net,plant}$	net plant power (W)
$\dot{W}_{sc}$	steam cycle modified power (W)
$\dot{W}_{st}$	steam turbine gross power (W)
Δp	pressure drop (bar)
Δp_{hrsg}	gas-side HRSG pressure drop (bar)

ΔT_{cw}	cooling water temperature difference (K)
ΔT_{pinch}	pinch-point temperature difference (K)
$\eta_{net,plant}$	net plant efficiency (-)
σ	standard deviation
Φ	parent population
CPSO	constrained particle swarm optimizer
GA	genetic algorithm
GSS	generating set search
GT	gas turbine
HRSC	heat recovery steam cycle
HRSG	heat recovery steam generator
MO	multi-objective
NSGA-II	non-dominated sorting genetic algorithm II
OTSG	once-through heat recovery steam generator
PSO	particle swarm optimizer
SC	steam cycle
ST	steam turbine
VGV	variable guide vane

1. Introduction

Today's offshore oil and gas installations are mostly powered by simple cycle gas turbines (GTs). To counter the cost of CO_2 emissions in Norway (taxes and quota), an alternative to a simple cycle configuration could be a combined cycle plant to increase the plant's efficiency and decrease the CO_2 emitted per generated kWh. A steam bottoming cycle, as part of a combined cycle, needs to be simple, with low weight and volume, on an offshore oil and gas installation [1]. On a small scale, a few offshore installations have combined cycles installed [2]. A 2013 increase in the CO_2 tax by the Norwegian parliament may make combined cycles more attractive for the future on the Norwegian continental shelf [3].

One of the keys to the implementation of combined cycles on offshore oil and gas installations is for the steam bottoming cycle to have a low weight-to-power ratio. For the remainder of this paper, the steam bottoming cycle will be referred to as the heat recovery steam cycle (HRSC). The HRSC consists of a heat recovery steam generator (HRSG), a steam turbine, a condenser, various pumps, a water treatment unit, and associated auxiliaries. While the design criteria for maximizing the HRSC power and efficiency are well-known [e.g., see 4], those for minimizing the weight-to-power ratio are still unclear. Previous studies of off-shore HRSC installations are based on knowledge-based designs relying on previous experience, literature search, and experts' opinions as exemplified in [5]. The knowledge-based design methodology is described in [6].

Direct-search algorithms are widely used in engineering when the objective function is a black-box, e.g., a sequential flowsheet simulation code, or a solver of differential-algebraic equations. Black-box optimizers do not make use of derivative information (they are also called derivative-free methods) as the black-box function may be non-differentiable, discontinuous, not defined in some points of the feasible space, and affected by numerical noise. Well-known examples of such methods are the Simplex method [7], the Pattern Search Algorithm [8], the Particle Swarm Optimizer (PSO) [9], and the several Genetic Algorithms (GAs) developed since the 1960s. A review and benchmarking of methods can be found in [10] for unconstrained and bound-constrained problems, and in [11] for nonlinearly constrained problems. Thanks to their robustness regarding numerical issues, such as numerical noise and discontinuities in the objective function, black-box methods have been successfully applied to several process engineering problems since the early 1970s, including steam cycles [12] integrated HRSCs [13], and steam generators [14].

More recently, engineering problems with different possible decision criteria (e.g., minimum weight or cost versus maximum power or efficiency), in which it is not easy to identify a single objective function, are often formulated and tackled as Multi-Objective (MO) optimization problems by means of evolutionary algorithms [15]. Instead, as for single-objective methods, such as the above mentioned direct-search methods, which return a single solution, evolutionary MO algorithms aim at determining the so-called Pareto frontier, i.e., a set of the most interesting solutions. Indeed, by definition of Pareto-optimality, no feasible solution gives better objective function values than a Pareto-optimal solution for at least one of the objective functions. For example, given two objective functions, f_1 and f_2 (e.g., power and weight), if the solution $\mathbf{x}$ is Pareto-optimal, no feasible solutions exist with the same value of f_1 and a better objective function value of f_2 and vice versa. Compared to the single solution returned by a single-objective optimizer, knowing the Pareto frontier is very useful in practice because: 1) it indicates not just one but a space of good solutions, allowing the designer to select the solution which best matches the installation constraints; 2) it graphically plots the trade-off between the different objectives (e.g., the gain of power which could be achieved by increasing the weight by a certain amount); and 3) it is possible to derive general criteria by analyzing the features of the Pareto-optimal solutions. As a consequence, MO algorithms have been extensively applied to the design of

HRSCs in dual-pressure [16] and other combined cycles [17], Organic Rankine Cycles on offshore platforms [18] and for low grade waste heat [19], and novel energy systems [20].

The aims of this work were to find the minimum weight-to-power ratio for a heat recovery steam cycle designed for offshore oil and gas installations, and to determine the trade-off between weight and power. These aims were to be achieved while utilizing a commercial process simulator with detailed process models within an optimization framework. In more detail, a process model of a single pressure level combined cycle was coupled with MATLAB [21] and used as a 'black-box' function by specific optimization algorithms. The process model computed the combined cycle performance and weight for fixed HRSC design variables, which were set by the MATLAB optimizer. Within this framework, firstly PGS-COM, the direct-search algorithm proposed by Martelli et al. in [22] and described in detail in [11], was used to determine the solution with minimum weight-to-power ratio; then NSGA-II, the multi-objective optimizer described in [23], was applied to identify the Pareto frontier of solutions with maximum power and minimum weight.

2. Methodology

2.1. Process description

The layout for the combined cycle was based on one GT (GE LM2500+G4), one single-pressure once-through heat recovery steam generator (OTSG), one steam turbine (ST), and a deaerating condenser, as shown in Fig. 1. This setup is explained in more detail in [5] (layout c). The GT was equipped with dry low emission burners and variable guide vanes (VGVs). The use of VGVs for marine combined cycles is further described in [24]. Process model assumptions are listed in Table 1. The HRSG designed for an offshore oil and gas installation including design parameter selection is discussed in [1]. Model validation of the knowledge-based design, which was the starting point for the optimization, was performed in [5]. For the gas turbine, the exhaust mass flow rate was constant at 90 kg/s for all design cases, whereas the turbine outlet temperature varied slightly (530–534 °C) due to changes in HRSG pressure loss.

2.2. Model description

GT PRO (design), GT MASTER (off-design), and PEACE (preliminary engineering and cost estimation) by Thermoflow Inc. were the software used for the combined cycle process modeling, simulations, and weight estimations [25]. Within the Thermoflow package, the IAPWS-IF97 water and steam properties were used [26]. The gas-side heat transfer convective correlations were based on ESCOA® [27].

GT PRO solves the heat and mass balance of the power plant and then uses the results to design the HRSG and the rest of the HRSC that can implement this. Certain design selections, such as number of pressure levels, type of HRSG, and condenser type, are chosen by the user. Material selection, tube configuration, and fin type in the HRSG can also be altered by the user as listed in Table 1. For the

condenser, GT PRO will select tube material (Titanium for seawater) and cleanliness (80% for seawater) based on the cooling water type and will choose tube diameter and thickness of standard sizes, water velocity, and number of passes in such a way as to produce a condenser of reasonable design and geometry [25].

The focus of the work outlined in this paper was to optimize the important process variables to achieve a low weight-to-power ratio. The process variables (optimization decision variables) selected, as listed in Table 2, were the ones which had a larger effect on the HRSC power, weight, or both. One can argue that the optimization should have been done with cost as an objective function. The reason for omitting cost in this study was that the cost for offshore installations is very project-specific.

The optimization was accomplished by linking MATLAB and GT PRO as displayed in Fig. 2. Microsoft Excel was used as an interface between the MATLAB and Thermoflow software. The single-objective optimization method used in this work was PGS-COM [11] and is further described in Section 2.3. For the multi-objective optimization, the NSGA-II was used [23], which is further described in Section 2.4.

2.2.1. Definitions

This subsection defines the variables used in the model and in the following sections of the paper. The steam cycle modified power output was defined as:

$$\dot{W}_{sc} = \dot{W}_{st} - \dot{W}_{aux,sc} - \Delta\dot{W}_{gt} \tag{1}$$

where $\dot{W}_{st}$ is the steam turbine gross power (the electrical output at the steam turbine generator terminals), $\dot{W}_{aux,sc}$ the steam cycle auxiliary power including boiler feedpump, condensate forwarding pump, cooling water pump, and miscellaneous steam turbine auxiliaries. $\Delta\dot{W}_{gt}$ is the difference in the gas turbine output at the generator terminals from that of the knowledge-based design. The last term was included to take into account changes in gas turbine power output due to changes in HRSG gas-side pressure drop. Considering only the net power of the steam cycle was not sufficient since the gas turbine power also was affected by changes in the HRSG design.

The net plant power output was defined as:

$$\dot{W}_{net,plant} = \dot{W}_{gt} + \dot{W}_{st} - \dot{W}_{aux} \tag{2}$$

where $\dot{W}_{gt}$ is the gas turbine gross power and $\dot{W}_{aux}$ the plant auxiliary power requirement.

The net plant efficiency was defined as:

$$\eta_{net,plant} = \frac{\dot{W}_{net,plant}}{(\dot{m}LHV)_{ng}} \tag{3}$$

where $\dot{m}_{ng}$ is the natural gas mass flow entering the system and LHV_{ng} the lower heating value of the natural gas.

For the off-design analyses, part load operational points were based on relative gas turbine load:

$$RL_{gt} = \frac{\dot{W}_{gt}}{\dot{W}_{gt,d}} \tag{4}$$

$\dot{W}_{gt,d}$ is here the gas turbine gross power output at design conditions.

CO_2 emitted from the power plant was defined as:

$$CO_2\ emitted = \frac{\dot{m}_{CO_2}}{\dot{W}_{net,plant}} \tag{5}$$

where $\dot{m}_{CO_2}$ is the mass flow of carbon dioxide emitted from the plant.

The weight-to-power ratio of the steam bottoming cycle was defined as:

$$W/P = \frac{m_{sc}}{\dot{W}_{sc}} \tag{6}$$

where m_{sc} is the total mass of all the included components in the steam cycle. Included in the weight estimations were steam turbine, generator, condenser, and heat recovery steam generator with stack. These weights were considered to be variable. A constant bulk weight was added to the equipment weight to include water storage tank, water treatment system, pumps, and skid structure. The bulk weight was, in this work, considered constant and would therefore not vary between the different designs. The wet weight, i.e., including the H_2O in the system, was used.

2.3. Single-objective optimization

The plant model described in Section 2.2 was used as a black-box function within the following optimization problem with the aim of minimizing the HRSC weight-to-power ratio:

- Objective: minimize the HRSC weight-to-power ratio W/P.
- Decision variables: superheated steam temperature T_{steam}, steam evaporation pressure p_{steam}, HRSG pinch point temperature difference ΔT_{pinch}, HRSG gas-side pressure drop Δp_{hrsg}, condenser pressure p_{cond}, condenser cooling water temperature difference ΔT_{cw}.
- Constraints: the decision variables are bounded as indicated in Table 2.

The lower and upper bounds of the decision variables, as displayed in Table 2, were selected on the basis of general technical limitations and practical limitations built into the GT PRO design tool. In more detail, the upper bound on T_{steam} was fixed by the gas turbine outlet temperature, while the lower bound was set to guarantee a reasonably high steam quality at the steam turbine outlet. The lower bound on p_{cond} was set according to the typical limitations of the vacuum and sealing systems, while the upper bound was set to a reasonably high value (so as not to exclude optimal solutions). The bounds on p_{steam} were set on the basis of a preliminary sensitivity analysis. To avoid a very large and high weight solution, the lower

bounds of ΔT_{pinch} and Δp_{hrsg} were set according to Table 2. The upper bounds of ΔT_{pinch} and Δp_{hrsg} were limited by a GT PRO practical design limitation related to the HRSG gas mass flux (mass flow rate per unit of cross-sectional area). A high ΔT_{pinch} leads to a smaller heat transfer surface area which gives a high gas mass flux. Similarly, a high Δp_{hrsg} leads to a more compact design which in turn leads to a high gas mass flux. For the ΔT_{cw} upper bound, typical regulations for the maximum allowable rise in cooling water temperature were taken into account. The lower bound was selected to stay within a reasonable cooling water mass flow rate.

Additional constraints were not included in the optimization problem since all the physical equations (i.e., mass and energy balance equations) and technical limitations were enforced within the black-box (GT PRO model). It is worth noting that the objective function value may not be defined in some points of the feasible region defined by the bounds because the plant simulation code fails to return a feasible solution (either a technical limitation is not met or the GT PRO sequential calculation fails to reach convergence). Moreover, the objective function may also be non-smooth (non-differentiable or discontinuous). For these reasons, an effective and robust direct-search algorithm must be used.

Among the available direct-search methods, we selected PGS-COM, the hybrid method specifically developed for non-smooth black-box problems [11]. This algorithm combines the positive features of the Constrained Particle Swarm Optimizer (CPSO) [28], Generating Set Search (GSS) [29], and the Complex [30]. Each iteration of the algorithm consists of three steps: (i) a search step corresponding to a population update of a revised CPSO, (ii) an optional (skipped if the CPSO improves the best solution found so far) poll step (i.e., sampling of the objective function along a set of directions satisfying certain mathematical properties so as to guarantee the convergence to a stationary point) corresponding to an iteration of the GSS around the best solution found so far, and (iii) a few optional (skipped if either the CPSO or the GSS step finds a better solution) reflection steps corresponding to a few iterations of the Complex algorithm. The algorithm stops when the swarm size (defined as the maximum distance between the best particle and the remaining particles), the step size parameter of the GSS step and the size of the population used by the Complex step become smaller than the given threshold, or the maximum number of function evaluations is reached. The main idea is to exploit the effectiveness of the population-based CPSO algorithm to rapidly identify promising regions of the set of the feasible solutions, and then take advantage of the effectiveness of the Complex search for non-smooth problems to intensify the search in selected sub-regions. The GSS step is used to generate the starting solutions for the Complex step, and to improve the algorithm robustness towards numerical noise in the objective function (as GSS is more robust than Complex). The computational results presented in [11] indicate that, for noisy non-smooth black-box problems, PGS-COM performs better than 11 ad hoc methods. The parameter values of the algorithm (number of swarm particles, neighborhood size, minimum GSS step size parameter, etc.) in this work were the same as the values recommended in [11].

2.4. Multi-objective optimization

In this section, the methodology of the multi-objective optimization problem to determine the Pareto-optimal solutions (i.e., the Pareto frontier) with respect to minimum weight and maximum power is described:

- Objective 1: minimum weight.
- Objective 2: maximum power.
- Constraints: same as those for the single-objective problem.

Over the past decade, multi-objective evolutionary algorithms have been attracting growing attention from both method developers and engineers, and a large number of algorithms have been proposed [15]. This is mainly due to their ability to find multiple Pareto-optimal solutions (i.e., the Pareto frontier) in one single run. Among the several evolutionary algorithms to tackle the MO problem, we selected the Non-dominated Sorting Genetic Algorithm II (NSGA-II) [23] because it is quite effective on black-box problems [31], well-proven [17], and readily available within the MATLAB Global Optimization Toolbox [21].

The algorithm adopts the general idea of a genetic algorithm but with some changes. The algorithm starts with a random solution population Φ of size N_p. Then, the standard genetic algorithm operators (i.e., selection, crossover, and mutation) are used to create a child population Q from Φ with the same size N_p. More in detail, the binary tournament selection is applied to choose the parent solutions for reproduction, i.e., choosing a set of N_t solutions at random and then taking the best individual out of that set to be a parent. Child solutions are created according to the 'intermediate' crossover function, i.e., by taking a weighted average of the parents' solutions:

$$child_j = parent1_j + rand \cdot ratio \cdot (parent2_j - parent1_j) \tag{7}$$

where $child_j$ labels the j-th variable of the child's solution vector, $parent1_j$ and $parent2_j$ the j-th variable of the parents' solution vector, $rand$ indicates a random number between 0 and 1, and $ratio$ is a free tuning parameter to be set by the user. Finally, in order to search a broader space by providing genetic diversity to the child solutions, the Gaussian mutation operator is applied. It adds a random number taken from a Gaussian distribution with mean value equal 0 and standard deviation σ to each solution variable. It is worth noting that the standard deviation shrinks as generations go by.

Once N child populations are generated, the parent and child populations (thus $2N$ solutions) are sorted according to the principle of non-domination: given a minimization problem with $N_f > 1$ objective functions f, a solution (element of the population) $\mathbf{p}$ dominates another element $\mathbf{q} \in \Phi \cup Q$ if there exists at least one objective function i with $f_i(\mathbf{p}) < f_i(\mathbf{q})$, and $f_k(\mathbf{p}) \leq f_k(\mathbf{q})$ for all other k. Solutions are ranked by assigning each of them a fitness equal to its non-domination level. According to this criterion, elements with

no dominating elements have fitness equal to 1, those dominated only by elements with fitness equal to 1 have fitness equal to 2, and so on. For each fitness level, in order to preserve solution diversity and obtain a uniform Pareto frontier, elements are sorted according to the 'crowded-comparison criterion,' which gives preference to those solutions that have a larger distance from the others in the function space (thus, are far away on the Pareto frontier). Finally, the new population is generated by taking the first N_p elements of the sorted fitness levels. The process is repeated until either all elements of the population have fitness level equal to 1 (i.e., all solutions stay on the Pareto frontier) or a predetermined number of function evaluations are reached.

The NSGA-II parameter values, after preliminary computational tests, were selected as:

- Population size, $N_p = 50$
- Number of solutions for the selection function, $N_t = 4$
- *Ratio* parameter of the crossover function = 1
- *Scale* and *shrink* factors of the mutation function = 1
- Maximum number of *generations* = $1,000$

3. Results and discussion

3.1. Single-objective optimization

The objective function for the single-objective optimization was the HRSC weight-to-power ratio W/P.

One optimization required approximately 10,000 GT PRO simulations with a computational time of around 10 hours on a 2.4 GHz Intel Core i7-2760QM CPU (Quad-core).

The results are displayed in Table 3. Compared to the knowledge-based design, the optimized solution has variables leading to a lower weight of the HRSG (weight-wise the dominant component) while allowing for a larger steam turbine and condenser to achieve a higher steam cycle power output. The higher HRSG pinch-point temperature difference and the gas-side pressure drop for the optimized solution led to a smaller HRSG. The lower condensing pressure led to a higher power output and higher steam turbine and condenser weights.

The W/P was 4% lower than in the case of the knowledge-based design. The difference is small but not negligible. This difference could rise if hardware design (fin design, material selection, tubing design and layout, steam turbine design, condenser design) were also actively altered. Moreover, note that three of the six optimization variables were at their bounds: ΔT_{pinch}, Δp_{hrsg}, and ΔT_{cw}. This means that a further improvement of the W/P ratio could be achieved by relaxing these bounds and enlarging the feasible region. Assuming that the upper bound on ΔT_{cw} cannot be increased without violating environmental regulations,

only Δp_{hrsg} and ΔT_{pinch} could be increased. As explained in Section 2.3, these upper bounds were set by the GT PRO design criteria which tend to limit the gas mass flux across the HRSG sections.

3.1.1. Off-design operation

Off-design process simulations have previously been performed for the knowledge-based design [5]. On offshore oil and gas installations, part load operation is of high importance since the power plant has to follow the demand of the oil and gas processes. To be able to compare whether the optimized design showed an improved or a worse part load behavior, off-design simulations for the load range of 40–100% relative gas turbine load were completed using GT MASTER [25]. The results are shown in Fig. 3. The net plant efficiency difference between the two designs remains close to constant in the 40–100% load range.

3.2. Multi-objective optimization

Fig. 4 displays the objective function values of non-dominated solutions returned by the algorithm after 50,000 function evaluations (corresponding to 50,000 GT PRO simulations). Those solutions can be considered as an approximation of the Pareto front, although the front could be pushed lower (and pass through the point found by the single-objective optimizer) if more function evaluations were completed. However, practical limitations capped the maximum number of function evaluations (simulation runs) as the displayed Pareto front approximation took more than 60 hours. The knowledge-based design is also indicated in Fig. 4.

How do the parameters develop along the Pareto front? To the left in Fig. 4, for designs with a lower weight, the parameters are characterized by low ΔT_{cw}, and high p_{steam}, ΔT_{pinch}, Δp_{hrsg}, and p_{cond}. The solutions to the right in the figure show the opposite behavior of the process parameters. T_{steam} shows small variations in the range of 478–488 °C for all designs on the Pareto front. There are some commonalities for designs with a W/P lower than for the knowledge-based design ($W/P = 34.4$). Among the non-dominated solutions returned by the multiobjective algorithm, eight designs that have a lower W/P than 34.4 are shown in Fig. 5, where W/P is plotted as a function of the steam cycle weight. All the eight designs have a $\Delta p_{hrsg} > 28$ mbar and $p_{cond} < 0.07$ bar.

The parameter development was further emphasized by running two single-objective optimizations to complement the Pareto front. The first objective was to minimize the weight while staying within the lower and upper bounds of the parameters. The second objective was to maximize power output. The results from the two optimizations are shown in Table 4.

Two designs, A and B, highlighted in Fig. 5 show different designs with the same W/P. Designs A and B have significantly different process parameters, as displayed in Table 4, but result in the same W/P. Design A is a low weight/low power solution while design B is a solution with higher weight and power.

The selection of design could then be decided by the need for power or by the limitation of weight on the offshore installation.

The weight distribution of the components composing the variable weight in the designs along the Pareto front is shown in the stacked area diagram in Fig. 6. The eight designs with the lowest W/P are indicated by the box in Fig. 6.

4. Conclusions

Optimization of the design can open up new ways of thinking about the plant. A designer may have difficulty thinking outside the box, e.g., through being affected by existing designs and experts' opinion. This can be exemplified by the condenser pressure in this work. Existing designs in offshore oil and gas installations have a higher condenser pressure to keep the weight of the condenser lower. The knowledge-based design methodology, which is affected by previous designs, also selected a higher condenser pressure (0.07 bar). However, the optimizer designed the condenser to maximize the power of the steam cycle and instead focused the weight savings on the HRSG. The maximum W/P therefore had a low condenser pressure of 0.037 bar. The resulting W/P was 4% lower than in the knowledge-based design.

The results of the multi-objective optimization allow the engineer to select the solution which best matches the installation constraints, whether it be a design decided by the need for power or by the limitation of weight on the offshore installation. In general, the designs on the Pareto front, resulting from the multi-objective optimization, with W/P lower than the knowledge-based design showed a high gas-side HRSG pressure drop and a low condenser pressure. The live steam pressure was in a narrow range around 480 °C.

The work shows the feasibility of linking MATLAB and Thermoflow software. For future work, the optimization could be expanded to include detailed hardware design alterations, such as, fin design, tubing design and layout, and material selection. This was not possible with the Thermoflow version used (only possible via manual selection within the Thermoflow software). For future work, alternative geometries of the entire HRSG could also be envisioned for a more compact result. This could, e.g., include a cylindrical HRSG with helical-shaped coils.

5. Acknowledgments

Support from the Gas Technology Centre at NTNU-SINTEF helped achieve this collaborative effort. This publication forms a part of the EFFORT project, performed under the strategic Norwegian research program PETROMAKS. The authors acknowledge the partners Statoil, TOTAL E&P Norway, Shell Technology Norway, PETROBRAS, SINTEF Energy Research, NTNU-Norwegian University of Science and Technology, and the Research Council of Norway (203310/S60) for their support.

References

[1] L. O. Nord, O. Bolland, Steam bottoming cycles offshore—Challenges and possibilities, Journal of Power Technology 92 (3) (2012) 201–207.

[2] P. Kloster, Energy optimization on offshore installations with emphasis on offshore combined cycle plants, in: Offshore Europe Conference; Aberdeen, Scotland, Society of Petroleum Engineers Inc., 1999, paper no. SPE 56964.

[3] Ministry of the Environment, the Norwegian Government, Meld. St. 21 (2011–2012): white paper on climate efforts (2012).

[4] R. Kehlhofer, B. Rukes, F. Hannemann, F. Stirnimann, Combined-Cycle Gas & Steam Turbine Power Plants, 3rd Edition, PennWell Publishing Company, 2009, ISBN 978-1-59370-168-0.

[5] L. O. Nord, O. Bolland, Design and off-design simulations of combined cycles for offshore oil and gas installations, Applied Thermal Engineering 54 (1) (2013) 85–91.

[6] Y. Jaluria, Design and Optimization of Thermal Systems, 2nd Edition, CRC Press, 2008, ISBN 978-0-8493-3753-6.

[7] J. A. Nelder, R. Mead, A Simplex method for function minimization, The Computer Journal 7 (4) (1965) 308–313.

[8] R. Hooke, T. A. Jeeves, Direct search solution of numerical and statistical problems, Journal of the Association of Computing Machinery 8 (2) (1961) 212–229.

[9] J. Kennedy, R. Eberhart, Particle swarm optimization, in: Proceedings of IEEE International Conference on Neural Networks, Vol. 4, 1995, pp. 1942–1948.

[10] L. M. Rios, N. V. Sahinidis, Derivative-free optimization: A review of algorithms and comparison of software implementations, Journal of Global Optimization 56 (3) (2013) 1247–1293.

[11] E. Martelli, E. Amaldi, PGS-COM: A hybrid method for constrained non-smooth black-box optimization problems: Brief review, novel algorithm and comparative evaluation, Computers and Chemical Engineering 63 (2014) 108–139.

[12] T. R. Colmeranes, W. D. Seider, Synthesis of utility systems integrated with chemical processes, Industrial & Engineering Chemistry Research 28 (1) (1989) 84–93.

[13] E. Martelli, E. Amaldi, S. Consonni, Numerical optimization of heat recovery steam cycles: Mathematical model, two-stage algorithm and applications, Computers and Chemical Engineering 35 (12) (2011) 2799–2823.

[14] E. Martelli, T. Kreutz, M. Gatti, P. Chiesa, S. Consonni, Numerical optimization of steam cycles and steam generators designs for a coal to FT plant, Chemical Engineering Research and Design 91 (8) (2013) 1467–1482.

[15] A. Abraham, L. C. Jain, R. Goldberg, Evolutionary Multiobjective Optimization: Theoretical advances and applications, Springer, 2005, ISBN 978-1-85233-787-2.

[16] A. G. Kaviri, M. N. M. Jaafar, T. M. Lazim, Modeling and multi-objective exergy based optimization of a combined cycle power plant using a genetic algorithm, Energy Conversion and Management 58 (2012) 94–103.

[17] P. Ahmadi, I. Dincer, M. A. Rosen, Exergy, exergoeconomic and environmental analyses and evolutionary algorithm based multi-objective optimization of combined cycle power plants, Energy 36 (10) (2011) 5886–5898.

[18] L. Pierobon, T. V. Nguyen, U. Larsen, F. Haglind, B. Elmegaard, Multi-objective optimization of organic Rankine cycles for waste heat recovery: Application in an offshore platform, Energy 58 (2013) 538–549.

[19] J. Wang, Z. Yan, M. Wang, M. Li, Y. Dai, Multi-objective optimization of an organic Rankine cycle (ORC) for low grade waste heat recovery using evolutionary algorithm, Energy Conversion and Management 71 (2013) 146–158.

[20] M. Gassner, F. Maréchal, Methodology for the optimal thermo-economic, multi-objective design of thermochemical fuel production from biomass, Computers and Chemical Engineering 33 (3) (2009) 769–781.

[21] Global Optimization Toolbox, MathWorks, 2013.

[22] E. Martelli, E. Amaldi, A novel hybrid direct search method for constrained non-smooth black-box problems, Computer Aided Chemical Engineering 32 (2013) 295–300.

[23] K. Deb, A. Pratap, S. Agarwal, T. Meyarivan, Fast and elitist multiobjective genetic algorithm: NSGA-II, in: IEEE Transactions on Evolutionary Computation, Vol. 6, 2002, pp. 182–197.

[24] F. Haglind, Variable geometry gas turbines for improving the part-load performance of marine combined cycles - gas turbine performance, Energy 35 (2) (2010) 562–570.

[25] GT PRO, GT MASTER, and PEACE Version 22, Thermoflow Inc., 2012.

[26] W. Wagner, J. R. Cooper, A. Dittmann, J. Kijima, H. J. Kretzschmar, A. Kruse, R. Mareš, K. Oguchi, H. Sato, I. Stöcker, O. Šifner, Y. Takaishi, I. Tanishita, J. Trübenbach, T. Willkommen, The IAPWS industrial formulation 1997 for the thermodynamic properties of water and steam, Journal of Engineering for Gas Turbines and Power 122 (1) (2000) 150–180.

[27] ESCOA Fintube Manual, ESCOA Corp., Tulsa, OK, USA, 1979.

[28] X. Hu, R. Eberhart, Solving constrained nonlinear optimization problems with particle swarm optimization, in: Proceedings of the 6th World Multiconference on Systematics, Cybernetics and Informatics, 2002, pp. 203–206.

[29] R. M. Lewis, A. Shepherd, V. Torczon, Implementing generating set search methods for linearly constrained minimization, SIAM Journal of Scientific Computation 29 (6) (2007) 2507–2530.

[30] J. Andersson, Multiobjective Optimization in Engineering Design: Application to Fluid Power Systems, PhD thesis, Department of Mechanical Engineering, Linköping University, Sweden, 2001, ISBN 91-7219-943-1.

[31] A. L. Custódio, J. F. A. Madeira, A. I. F. Vaz, L. N. Vicente, Direct multisearch for multiobjective optimization, SIAM Journal on Optimization 21 (3) (2011) 1109–1140.

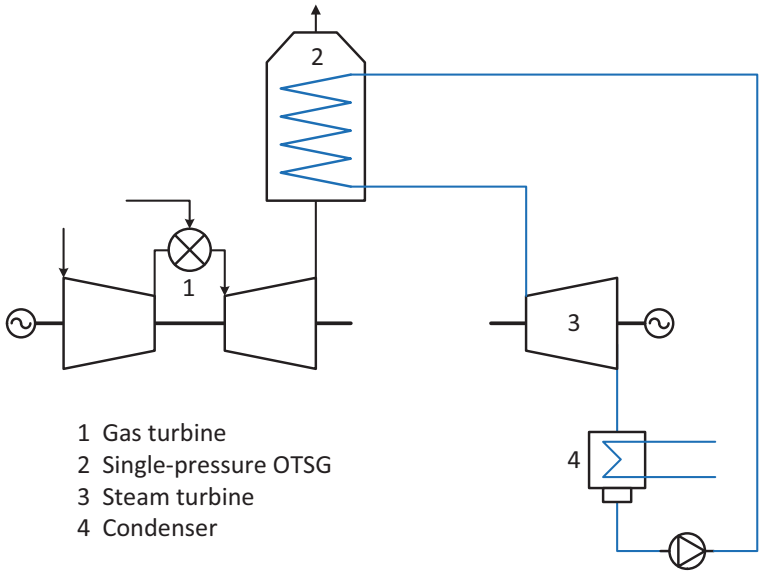

Figure 1: Layout of combined cycle for offshore oil and gas installations.

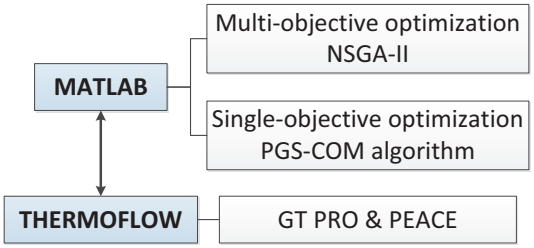

Figure 2: Overview of methodology. The Thermoflow model of the combined cycle is used by the MATLAB optimizer as a black-box function.

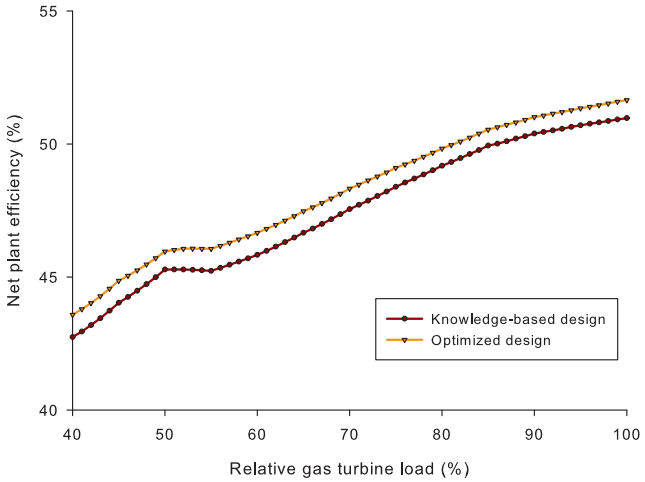

Figure 3: Comparison of the net plant efficiency at part load operation of the knowledge-based and optimized designs.

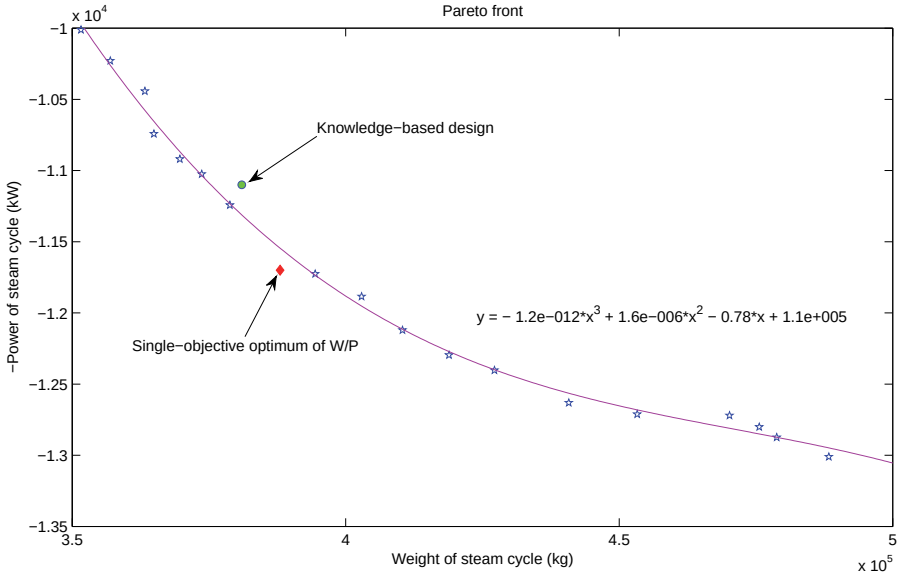

Figure 4: Pareto front with a cubic polynomial trend line. Knowledge-based design and single-objective optimum of W/P are indicated in plot.

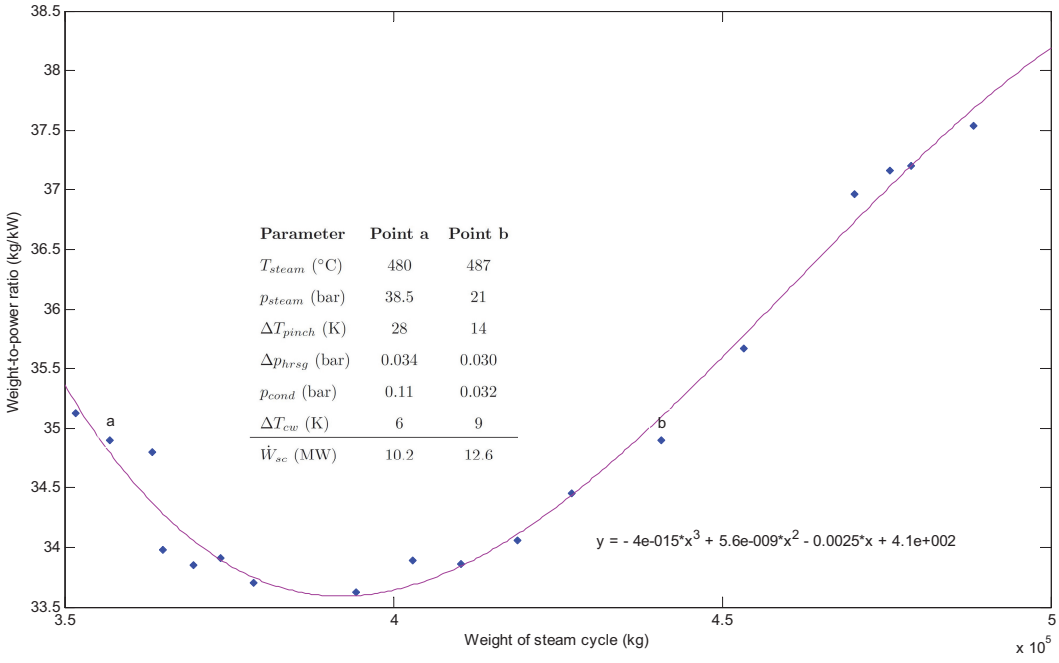

Parameter	Point a	Point b
T_{steam} (°C)	480	487
p_{steam} (bar)	38.5	21
ΔT_{pinch} (K)	28	14
Δp_{hrsg} (bar)	0.034	0.030
p_{cond} (bar)	0.11	0.032
ΔT_{cw} (K)	6	9
$\dot{W}_{sc}$ (MW)	10.2	12.6

Figure 5: Points of the Pareto front plotted as W/P as a function of steam cycle weight. Two designs (A, B) with the same W/P highlighted to illustrate differences in process parameters, as displayed in Table 4.

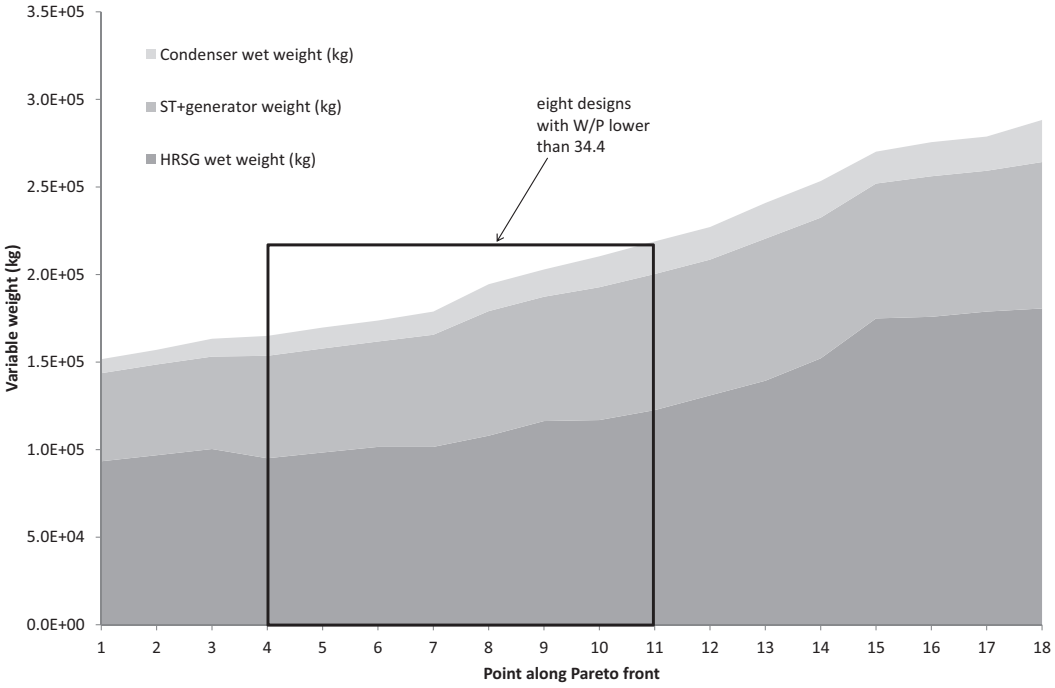

Figure 6: Distribution of variable weights along the Pareto front.

Table 1: Process model assumptions.

Site	
Ambient T (°C)	15
Ambient pressure (bar)	1.013
Ambient relative humidity (%)	60
Frequency (Hz)	60
Cooling water system	Direct water cooling
Cooling water	Sea water
Cooling water T (°C)	10
Gas turbine	
Model type	GE LM2500+G4
GT fuel	Methane
Lower heating value (kJ/kg)	50047
GT inlet Δp (bar)	0.010
HRSG	
Tube material	Incoloy
Fin material	TP 409
Fin type	Serrated
Tube layout	Staggered
Condenser	
Condenser type	Deaerating condenser
Heat exchanger design	Shell-and-tube

Table 2: Lower and upper bounds of optimization decision variables.

Variable	**Lower bound**	**Upper bound**
T_{steam} (°C)	400	510
p_{steam} (bar)	15	40
ΔT_{pinch} (K)	10	30
Δp_{hrsg} (bar)	0.015	0.035
p_{cond} (bar)	0.03	0.12
ΔT_{cw} (K)	3	10

Table 3: Comparison of knowledge-based and optimized designs. The objective function was the weight-to-power ratio.

	Knowledge-based design	**Optimized design**
T_{steam} (°C)	450	495
p_{steam} (bar)	25	24.5
ΔT_{pinch} (K)	25	30
Δp_{hrsg} (bar)	0.025	0.035
p_{cond} (bar)	0.07	0.037
ΔT_{cw} (K)	10	10
Plant net power (MW)	42.9	43.5
Plant net efficiency (%)	51.0	51.7
CO_2 emitted (kg/MWh)	387	382
GT gross power (MW)	32.1	31.9
ST gross power (MW)	11.3	12.0
SC modified power (MW)	**11.1**	**11.7**
Massflow steam (kg/s)	11.6	11.0
Weight wet HRSG (10^3 kg)	109	99
Weight ST+gen (10^3 kg)	60	73
Weight wet cond (10^3 kg)	12	16
Weight SC rest (10^3 kg)	200	200
Total SC weight (10^3 kg)	**382**	**388**
Weight-to-power ratio (kg/kW)	**34.4**	**33.2**

Table 4: Lowest weight and highest power solutions as well as two designs with the same W/P (designs A and B) to showcase the variable development along the Pareto front.

Parameter	**Minimum weight**	**Maximum power**	**Design A**	**Design B**
T_{steam} (°C)	415	510	480	487
p_{steam} (bar)	40	16.4	38.5	21
ΔT_{pinch} (K)	30	10	28	14
Δp_{hrsg} (bar)	0.035	0.015	0.034	0.030
p_{cond} (bar)	0.12	0.03	0.11	0.032
ΔT_{cw} (K)	5.9	10	6	9
$\eta_{net,plant}$ (%)	49.4	53.3	50.0	52.7
CO_2 *emitted* (kg/MWh)	399	370	395	374
$\dot{W}_{sc}$ (MW)	9.8	13.1	10.2	12.6
m_{sc} (10^3 kg)	349	499	358	440
W/P (kg/kW)	35.8	38.0	34.9	34.9